One-to-One and Three-to-One Internal Resonances in MEMS Shallow Arches

Hassen M. OUAKAD[1], Hamid M. SEDIGHI[2], Mohammad I. YOUNIS[3,4*],

[1]Department of Mechanical Engineering, King Fahd University of Petroleum and Minerals, Dhahran, 31261, KSA.
[2]Mechanical Engineering Department, Faculty of Engineering, Shahid Chamran University of Ahvaz, Ahvaz, IRI
[3]Mechanical Engineering Department, State University of New-York, Binghamton, 13850, NY, USA
[4]Physical Science and Engineering Division, King Abdullah University of Science and Technology, Thuwal, 23955-6900, KSA

([*]) Corresponding Author, Email: myounis@binghamton.edu

Abstract

The nonlinear modal coupling between the vibration modes of an arch shaped microstructure is an interesting phenomenon, which may have desirable features for numerous applications, such as vibration-based energy harvesters. This works presents an investigation into the potential nonlinear internal resonances of a Microelectromechanical systems (MEMS) arch when excited by static (DC) and dynamic (AC) electric forces. The influences of initial rise and mid-plane stretching are considered. The cases of one-to-one and three-to-one internal resonances are studied using the method of multiple scales and the direct attack of the partial differential equation of motion. It is shown that for certain initial rises, it is possible to activate a three-to-one internal resonance between the first and third symmetric modes. Also, using an anti-symmetric half-electrode actuation, a one-to-one internal resonance between the first symmetric and the second antisymmetric modes is demonstrated. These results can shed light on such interactions that are commonly found on micro and nano structures, such as carbon nano tubes.

Keywords: MEMS; Shallow Arch, one-to-one: three-to-one; internal resonance;

1. Introduction

Owing to their attractive features, significant research has been presented in recent years on miniaturized structures, such as micro/nano-electromechanical systems (M/NEMS) and Micro-Opto-Electro-Mechanical Systems (MOEMS) [1-8]. MEMS devices due to their small-size and high sensitivities are widely utilized in sensors and actuators [9], miniature gyroscopes

[10], micro-satellites [11], accelerometers [12], bio-MEMS [13], chemical sensors [14] and many other industrial applications. Among the most practical MEMS structures, arch shaped MEMS due to their interesting dynamics have been recently used as optical and digital mirrors, micro-relays, mechanical memories, [15] and micro-resonators [16]. These micro-scale structures show bi-stable behavior characterized by multi-valued curves in their load-deflection diagrams.

When beams are intentionally fabricated in a curved configuration, the phenomenon of snap-through can appear where the curved beam undergoes large deformation. Such structures can undergo snap-through behavior with large amplitude oscillation. Internal resonance can also interestingly occur in bistable structures with geometrical nonlinearity [17], such as in curved beams. Frequency response curves of bistable structures can have two separated multivalued ranges with two peaks bending to the left and right, respectively [18]. Das and Batra [19] examined the snap-through and the symmetry breaking of an arch shaped MEMS actuated by static and dynamic electrostatic forces and obtained the bifurcation diagrams for displacement-force curves. Ouakad [20] studied the dynamic behavior of a filter based on a doubly-clamped MEMS arch and excited the considered structure near its natural frequency by a combined DC and AC actuation loads. Alkharabsheh and Younis [21] investigated the influence of axial and electric forces on the dynamic response of initially curved MEMS arches and showed that the axial forces play an important role for tuning the natural frequency of such structures. By employing an analytic approach, Nayfeh and Emam [22] obtained the exact solution for the free vibrational behavior of buckled beams. They investigated the appearance of a 1:1 internal resonance of buckled beams by plotting the variation of the first natural frequencies versus the axial compressive load for the pre-buckled and post-buckled configurations. Nayfeh and

Balachandran [23] studied the response of internally resonant, two-degree-of-freedom systems coupled through quadratic non-linearity (including shallow arches). They have also considered few works on periodic, quasi-periodic and chaotic responses excited by external resonances or parametric resonances. The same group [24] have conducted an experimental investigation of the modal indications of composite structures and they have detected periodic and modulated motions.

Recent works have examined the impact of geometric and parametric nonlinearities on the transient dynamics and frequency response of curved MEMS devices under DC and AC actuations. Alkharabsheh and Younis [25] discussed the dynamics of an actuated MEMS shallow arches under the influence of flexible supports and examined the stability of the periodic responses captured by the Shooting method. Their simulation results experimentally demonstrated the existence of superharmonic resonances. Ouakad and Younis [26] presented the nonlinear dynamics of shallow arch micro-beams and showing the snap-through phenomenon as well as the softening and hardening behaviors near the first and third natural frequencies. By using the third-order shear deformation theory, Ghayesh et al. [27] presented the dynamic behavior and modal analysis of initially curved micro-plates including the small-scale effects. A recent study [28] was presented on the latching condition in electrostatically actuated curved beams based on a reduced-order modeling analysis. They demonstrated trapping the bistable beams at the latching point using a finite duration pulse.

Modes interaction represents an important topic for the dynamics of continuous systems, such as beams and plates. This phenomenon can be the consequence of the coupling between the system vibrational modes, therefore generating an internal resonance and energy exchange between the modes [29]. Such nonlinear interactions have been studied in numerous systems

ranging from macro, micro, and nano-scale [30-34]. These micro/nano structures have been shown to exhibit two-to-one [30-32], three-to-one [33], and one-to-one [34] internal resonances. More importantly, it has been proven that shallow arches allow the first and third frequencies to approach to each other as varying the initial curvature. Several groups have reported internal resonances of type one-to-one [35-37], two-to-one [38], and three-to-one [39, 40] for shallow arches and buckled beams.

One can note that few research efforts have methodically addressed the problem of internal resonances for MEMS arches under the nonlinear actuation electric forces. This investigation aims to thoroughly study the theoretical aspects of the one-to-one and three-to-one internal resonances for micromachined shallow arches, which can be found in many practical MEMS applications using MEMS arch configuration as its main moving structure.

2. Problem formulation

In this section, we define the problem governing the in-plane static and dynamic structural behavior of an electrically actuated shallow arch, Fig. 1a. ~~Hereafter, (ˆ) denotes dimensional quantities.~~ We consider a flexible doubly-clamped prismatic microbeam, Fig. 1b, of initial shape $\hat{w}_0(\hat{x}) = b_o[1 - cos(2\pi\hat{x}/L)]/2$, where b_o is the initial rise, of cross-section area A, and a second moment area $I = I_{\hat{y}\hat{y}}$. The beam is actuated by an electrostatic force assumed to have only a $\hat{z}$-component by a grounded electrode located underneath it and with an initial gap distance d in the $\hat{z}$ direction, Fig. 1b. It is assumed to be made of homogeneous isotopic elastic material with mass density ρ, Young's modulus E and Poisson's ratio ν. Since the width of microbeam is assumed larger than its thickness, we assume an effective modulus of elasticity $E_e = E/2(1-\nu^2)$.

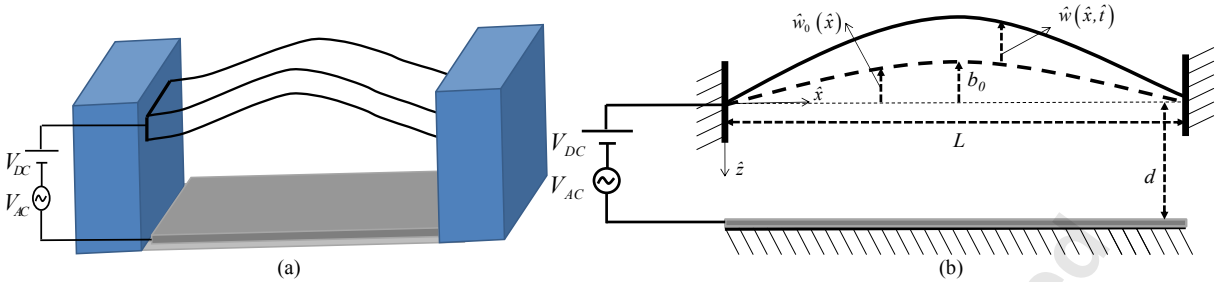

Fig. 1. (a) A 3-D and *(b)* a 2-D schematic of an electrically actuated MEMS shallow arch.

In this problem formulation, we assume a shallow arch, in which $\hat{w}_0' << 1$, where the "′" denotes the derivative with respect to $\hat{x}$. Hence, when actuated by electrostatic forces, the parallel-plates assumption can be considered valid. In another word, the axial component of the electrostatic force, due to the upper deformed electrode (the arch), is assumed negligible. This assumption, however, may not be valid for deep arches. The shallow arched microbeam is free to deflect in the $(\hat{x},\hat{z})$ plane, while its clamped ends are constrained in both the lateral $\hat{z}$ and axial $\hat{x}$ directions by the fixed anchors. Therefore, assuming an Euler-Bernoulli beam model, the nonlinear equation of motion governing the transverse deflection $\hat{w}(\hat{x},\hat{t})$ of the arch of width b, thickness h, and length L can be expressed as [29]

$$E_e I\frac{\partial^4\hat{w}}{\partial\hat{x}^4}+\rho A\frac{\partial^2\hat{w}}{\partial\hat{t}^2}+\tilde{c}\frac{\partial\hat{w}}{\partial\hat{t}}=\frac{\hat{E}'\hat{A}}{2\hat{L}}\left[\frac{\partial^2\hat{w}}{\partial\hat{x}^2}+\frac{\partial^2\hat{w}_0}{\partial\hat{x}^2}\right]\left[\int_0^{\hat{L}}\left\{\left(\frac{\partial\hat{w}}{\partial\hat{x}}\right)^2+2\left(\frac{\partial\hat{w}}{\partial\hat{x}}\frac{\partial\hat{w}_0}{\partial\hat{x}}\right)\right\}d\hat{x}\right]-\hat{F}_{electric}\left(\hat{w},V_{DC},V_{AC}\right), \quad (1)$$

where the function $\hat{F}_{electric}\left(\hat{w},V_{DC},V_{AC}\right)$, represents the distributed electrostatic force per unit length arising between the two parallel electrodes, the curved microbeam and its lower stationary actuating electrode, respectively. Neglecting the electric fringing-fields effect, the electrostatic force per unit length of the beam can be approximated as [42, 43]

$$\hat{F}_{elect}\left(\hat{w},V_{DC}\right)=\frac{\varepsilon_0 b\left(V_{DC}+V_{AC}\cos(\tilde{\Omega}\hat{t})\right)^2}{2\left(\hat{W}(\hat{x},\hat{t})\right)^2}, \tag{2}$$

where $\hat{W}(\hat{x},\hat{t})=d+\hat{w}_0(\hat{x})+\hat{w}(\hat{x},\hat{t})$, and where $\varepsilon_0=8.854\times10^{-12}$ F.m^{-1}, is the permittivity of free space and $V_{\rm DC}$ and $V_{\rm AC}$ are the DC static and AC harmonic voltages, respectively, applied between the moving arched electrode and its stationary lower electrode, both initially separated by a gap distance of $d+\hat{w}_0(\hat{x})$.

The respective boundary conditions are:

$$\hat{w}\left(0,\hat{t}\right)=0,\quad \frac{\partial\hat{w}}{\partial\hat{x}}\left(0,\hat{t}\right)=0,\quad \hat{w}\left(L,\hat{t}\right)=0,\quad \frac{\partial\hat{w}}{\partial\hat{x}}\left(L,\hat{t}\right)=0, \tag{3}$$

For convenience, we introduce the following nondimensional variables:

$$w=\frac{\hat{w}}{d},\qquad w_0=\frac{\hat{w}_0}{d},\qquad x=\frac{\hat{x}}{L},\qquad t=\frac{\hat{t}}{T}, \tag{4}$$

where T is a time constant defined by $T=\sqrt{\rho AL^4/E_eI}$.

Consequently, the normalized equations of motion and associated boundary conditions can be written as:

$$\frac{\partial^4 w}{\partial x^4}+\frac{\partial^2 w}{\partial t^2}+c\frac{\partial w}{\partial t}=\alpha_1\left[\frac{\partial^2 w}{\partial x^2}+\frac{d^2 w_0}{dx^2}\right]\left[\int_0^1\left\{\left(\frac{\partial w}{\partial x}\right)^2+2\left(\frac{\partial w}{\partial x}\frac{dw_0}{dx}\right)\right\}dx\right]-\alpha_2 F_e, \tag{5}$$

$$w\left(0,t\right)=0,\quad \frac{\partial w}{\partial x}\left(0,t\right)=0,\quad w\left(1,t\right)=0,\quad \frac{\partial w}{\partial x}\left(1,t\right)=0, \tag{6}$$

where

$$w_0(x)=\frac{b_o}{2d}[1-\cos(2\pi x)],\quad F_e=\frac{[V_{DC}+V_{AC}\cos(\Omega t)]^2}{\left(1+w_0+w\right)^2},$$
$$\alpha_1=6\left(\frac{d}{h}\right)^2,\quad \alpha_2=\frac{\varepsilon_0 bL^4}{2E_e Id^3},\quad \Omega=\frac{\tilde{\Omega}}{\omega_n},\quad \omega_n=\sqrt{E_e I/\rho AL^4},\quad c=\frac{\tilde{c}L^4}{E_e IT}, \tag{7}$$

3. Perturbation Analysis

Internal resonance between two modes occurs when there is an integer relationship between their respective natural frequencies. This form of resonance may occur only in multi-degree-of-freedom systems with some form of nonlinearity [44]. When internal resonance exists simultaneously with an external resonance, it is often referred to as autoparametric resonance [44, 45]. In some cases this resonance depends on the geometry, composition, and boundary conditions of the system. Nayfeh and Mook [46] stated that when internal resonance exists in a free system, there often exists some sort of energy exchange among the modes involved in that resonance.

As a case study, we consider a Polysilicon clamped-clamped shallow of *L=1000μm, h=2.4μm, b=30μm*, and initial gap size of *d=10.1μm*. Since the system under investigation has quadratic and cubic nonlinearities, internal resonance can occur. In order to ascertain this possibility of mode interactions, we first solve the linear undamped vibration problem of the shallow arch under zero actuation and while varying its initial maximum rise value. For this, we solve the eigenvalue problem associated with the nonlinear beam equation, Eq. (5) [9]. First, a reduced-order model (ROM) of Eq. (5) based on the Galerkin procedure is derived. Then, after neglecting damping and the nonlinear electric force, we obtain the Jacobian matrix of the system by applying a Taylor series expansion around the equilibrium position. Finally, to calculate the natural frequencies of the shallow arch for a given initial rise, we calculate the eigenvalues of the

Journal of Computational and Nonlinear Dynamics. Received November 08, 2016;
Accepted manuscript posted May 24, 2017. doi:10.1115/1.4036815

Jacobian Matrix, and then by taking the magnitudes of each individual eigenvalue, we obtain the natural frequencies of the system. Figure 2 shows the effect of varying the initial rise of the arch on its first three natural frequencies. Looking carefully at Fig. 2, and zooming around the first three natural frequencies, we can see clearly the possibility to have a one-to-one internal resonance between the first symmetric and second antisymmetric modes at b_0=6.32 μm and a three-to-one internal resonance between the first symmetric and third symmetric modes at b_0=3.44 μm. Table 1 shows plots for the modeshapes of the first, second and third natural frequencies at selected values of initial rises. One can see that the first and third mode change slightly while the second mode remains unchanged with the rise level. A final note to be mentioned here is that the first frequency value is almost equal to the second one at around b_0=6.32 μm offering a possibility of internal resonances between the modes. In addition, at around b_0=3.44 μm, the first and third mode, both of symmetric shapes, are having their linear natural frequencies to be almost commensurate (ω_3=127.933≈**3*** ω_1) and hence suggesting another possibility of an internal resonance.

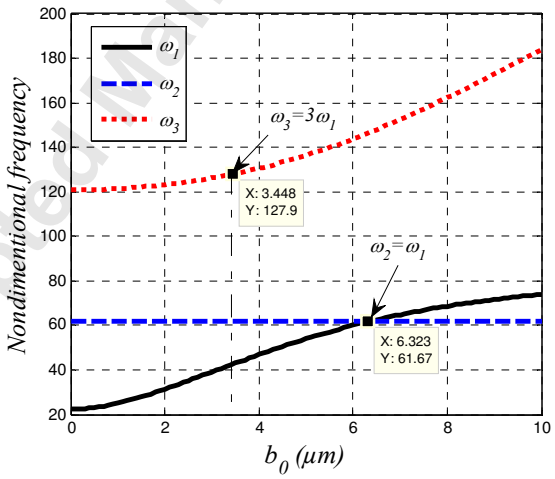

Fig. 2: The variation of the first three natural frequencies with the initial rise b_0 of the shallow arch and the possibility of internal resonances.

Journal of Computational and Nonlinear Dynamics. Received November 08, 2016;
Accepted manuscript posted May 24, 2017. doi:10.1115/1.4036815

Table 1: The simulated modeshapes of the first three in-plane modes for various arch initial rise levels

	First Mode	Second Mode	Third Mode
b_0=0 μm	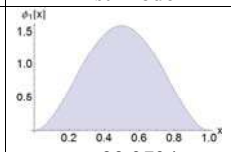 ω_1 =22.3734	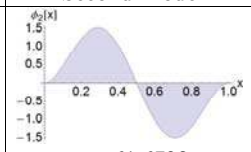 ω_2 =61.6728	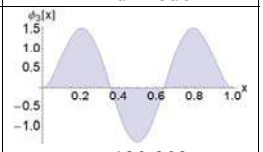 ω_3=120.903
b_0=2 μm	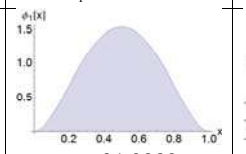 ω_1 =31.3389	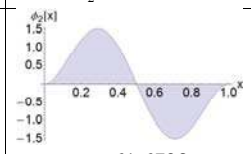 ω_2 =61.6728	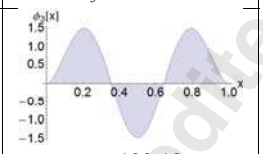 ω_3=123.18
b_0=3.448 μm	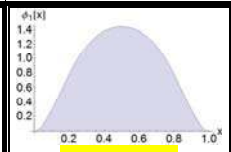 ω_1 =42.6325	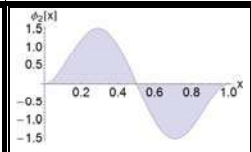 ω_2 =61.6728	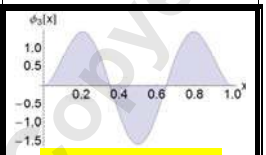 ω_3=127.933≈**3*** ω_1
b_0=5 μm	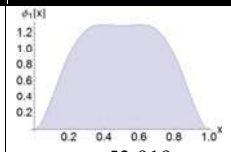 ω_1 =53.919	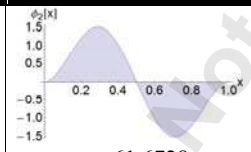 ω_2 =61.6728	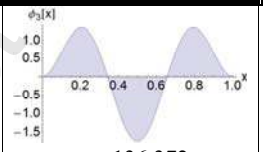 ω_3=136.372
b_0=6.323 μm	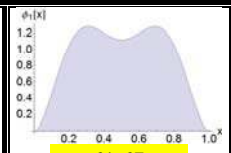 ω_1 =61.67≈ ω_2	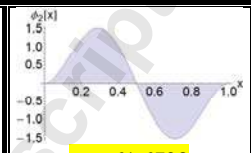 ω_2 =61.6728	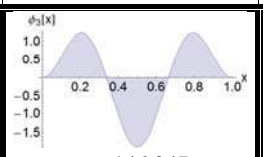 ω_3=146.347
b_0=8 μm	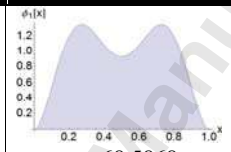 ω_1 =68.5868	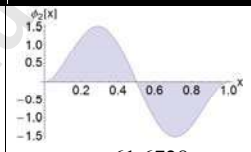 ω_2 =61.6728	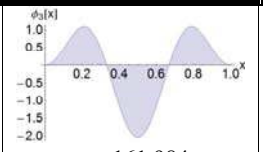 ω_3=161.984

Subsequently, we apply the method of multiple scales with the direct attack of the equations of motion, Eqs. (5) and (6) [47]. The details of the procedure can be found in Appendix A. To this end, we seek a solution in the form

$$w(x,t,\varepsilon) = w_s(x) + u(x,t) \tag{8}$$

where w_s is the static component of the arch deflection and u is its dynamic component.

For both types of investigated internal resonances, the perturbation analysis yields, to the first-order approximation, the following response of the MEMS arch to the DC and AC harmonic excitation:

$$w(x,t) = w_s(x) + a_n \cos(\omega_n t + \beta_n)\phi_n(x) + a_m \cos(\omega_m t + \beta_m)\phi_m(x) + \ldots \tag{9}$$

where ω_n, ω_m and $\phi_n(x)$, $\phi_m(x)$ are the natural frequencies and corresponding eigenfunctions for the n^{th} and m^{th} modes, respectively, and $a_n, \beta_n, a_m, \beta_m$ are real-valued functions, representing, the amplitude and phase of the response of the n^{th} and m^{th} mode, respectively, which are obtained from the results of the perturbation analysis (see Appendix A).

i) Three-to-one internal resonance

For this case, the application of the method of multiple scales yields the following modulation equations governing the amplitude and phase of the two involved n^{th} and m^{th} modes:

$$a_n' = -\hat{c}\frac{1}{2}a_n - \frac{\Lambda_n}{8\omega_n}a_m^3 \sin(\gamma_1), \tag{10}$$

$$a_n(\gamma_1' - 3\gamma_{2m}') = a_n(\sigma_1 - 3\sigma_2) - \frac{S_{nn}}{8\omega_n}a_n^3 - \frac{S_{nm}}{8\omega_n}a_n a_m^2 - \frac{\Lambda_n}{8\omega_n}a_m^3 \cos(\gamma_1), \tag{11}$$

$$a_m' = -\hat{c}\frac{1}{2}a_m + \frac{\Lambda_m}{8\omega_m}a_n a_m^2 \sin(\gamma_1) + \frac{f_m}{\omega_m}\sin(\gamma_{2m}), \tag{12}$$

$$a_m\gamma_{2m}' = -a_m\sigma_2 + \frac{S_{mm}}{8\omega_m}a_m^3 + \frac{S_{mn}}{8\omega_m}a_m a_n^2 + \frac{\Lambda_m}{8\omega_m}a_n a_m^2 \cos(\gamma_1) + \frac{f_m}{\omega_m}\cos(\gamma_{2m}), \tag{13}$$

where

$$\gamma_1 = \sigma_1 T_2 - 3\beta_m + \beta_n, \text{ and } \gamma_{2m} = \sigma_2 T_2 - \beta_m, \ \omega_n = 3\omega_m + \varepsilon^2\sigma_1, \text{ and } \ \Omega = \omega_m + \varepsilon^2\sigma_2 \tag{14}$$

S_{ij} and Λ_i represent the modal interaction coefficients, as defined in Eqs. (A29-A31) in Appendix A, and the rest of functions, such as the forcing coefficient f_i are defined in Eq. (A28) in Appendix A.

ii) One-to-one internal resonance

For this case, the application of the method of multiple scales yields the following modulation equations governing the amplitude and phase of the two involved *n*th and *m*th modes:

$$a_n' = -\frac{\hat{c}}{2}a_n - \frac{R_1}{8\omega_n}a_m^3\sin(\gamma_1) - \frac{R_2}{8\omega_n}a_n^2 a_m\sin(\gamma_1) + \\ -\frac{R_3}{8\omega_n}a_m^2 a_n\sin(2\gamma_1) + \frac{R_4}{8\omega_n}a_n^3\sin(\gamma_1); \tag{15}$$

$$a_n(\gamma_1' - \gamma_{2m}') = a_n(\sigma_1 - \sigma_2) - \frac{S_{nn}}{8\omega_n}a_n^3 - \frac{S_{nm}}{8\omega_n}a_n a_m^2 - \frac{R_1}{8\omega_n}a_m^3\cos(\gamma_1) + \\ -\frac{R_2}{8\omega_n}a_n^2 a_m\cos(\gamma_1) - \frac{R_3}{8\omega_n}a_m^2 a_n\cos(2\gamma_1) - \frac{R_4}{8\omega_n}a_n^3\cos(\gamma_1); \tag{16}$$

$$a_m' = -\frac{\hat{c}}{2}a_m + \frac{R_5}{8\omega_m}a_n^3\sin(\gamma_1) + \frac{R_6}{8\omega_m}a_m^2 a_n\sin(\gamma_1) + \\ -\frac{R_7}{8\omega_m}a_n^2 a_m\sin(2\gamma_1) + \frac{R_8}{8\omega_m}a_m^3\sin(\gamma_1) + \frac{f_m\delta_{im}}{\omega_m}\sin(\gamma_{2m}); \tag{17}$$

$$a_m\gamma_{2m}' = -a_m\sigma_2 - \frac{S_{mm}}{8\omega_m}a_m^3 - \frac{S_{mn}}{8\omega_m}a_m a_n^2 - \frac{R_5}{8\omega_m}a_n^3\cos(\gamma_1) - \frac{R_6}{8\omega_m}a_m^2 a_n\cos(\gamma_1) + \\ -\frac{R_7}{8\omega_m}a_m^2 a_n\cos(2\gamma_1) - \frac{R_8}{8\omega_m}a_n^2 a_m\cos(\gamma_1) - \frac{f_m\delta_{im}}{\omega_m}\cos(\gamma_{2m}); \tag{18}$$

where:

$$\gamma_1 = \sigma_1 T_2 - \beta_m + \beta_n, \quad \gamma_{2m} = \sigma_2 T_2 - \beta_m, \quad \omega_n = \omega_m + \varepsilon^2\sigma_1, \text{ and } \Omega = \omega_m + \varepsilon^2\sigma_2 \tag{19}$$

S_{ij} and R_i represent the modal interaction coefficients, as defined in Eqs. (A29-A31), and Eq. (A44), respectively in Appendix A, and the rest of functions, such as the forcing coefficient f_i are defined in Eq. (A28) in Appendix A.

4. Numerical Results

Here, we first solve the boundary-value problems, Eqs. (A14)-(A18). Then, we evaluate numerically the integrals in Eqs. (A29)-(A31) and Eq. (A44) for the three-to-one and one-to-one internal resonance cases, respectively.

i) Three-to-one internal resonance

For the case of three-to-one internal resonance, we first compare our results to those published in [47] about the possibility of activation of three-to-one internal resonance between the first symmetric and second antisymmetric modes for an electrically actuated straight microbeam. In Table 2 (for the case of b_0=0 μm), we show the results of the computations of the interaction coefficients (Λ_i) for the case study of [47]. We can see clearly that those coefficients are identically zero for this case. Hence, even though the ratio between the natural frequencies is of three-to-one type, the considered modes suspected to be involved in an internal resonance are not coupled in the nonlinear sense and hence cannot exchange energy [44].

As a second case, we consider the possibility of three-to-one internal resonance between the first symmetric mode and the third symmetric mode of the arch when b_0= 3.44 μm, Fig. 2. We can see from Table 2, that the interaction coefficients (Λ_i) are nonzero for this particular case, offering the possibility to have nonlinear interaction between the considered modes.

Table 2: The interaction coefficients S_{ij} and Λ_i for the case of three-to-one internal resonance between the m^{th} and n^{th} modes.

m	n	b_0 (μm)	S_{mm}	S_{nn}	S_{mn}	S_{nm}	Λ_m	Λ_n
1	3	0	-1.59×10^{3}	-2.34×10^{4}	-4.04×10^{3}	-4.04×10^{3}	7.408×10^{-7}	-7.810×10^{-7}
1	3	3.44	9.34×10^{4}	1.73×10^{4}	3.75×10^{5}	3.75×10^{5}	-2.51×10^{4}	-8.4×10^{3}

To simulate the dynamics of the system, a long-time integration of the nonlinear beam equation of motion can be used. Nevertheless, this numerical method suffers convergence problems essentially in the neighborhood of bifurcations/instabilities and therefore is not

Journal of Computational and Nonlinear Dynamics. Received November 08, 2016;
Accepted manuscript posted May 24, 2017. doi:10.1115/1.4036815

considered a robust method for studying nonlinear vibrations. This is one of the motivations to use the method of multiple scales. This method can obtain periodic solutions and at the same time can analyze the stability of the solutions and identify the types of the bifurcation points. This method will be used in conjunction with the Jacobian matrix stability theory to study the stability of the captured periodic orbits. It is worth mentioning here that the stability of each solution obtained using the method of multiple scales is determined by examining the eigenvalues of the Jacobian matrix of Eqs. (A32)-(A35), for the case of three-to-one internal resonance, and Eqs. (A39)-(A42), for the case of one-to-one internal resonance, evaluated in both cases at each corresponding solution [48].

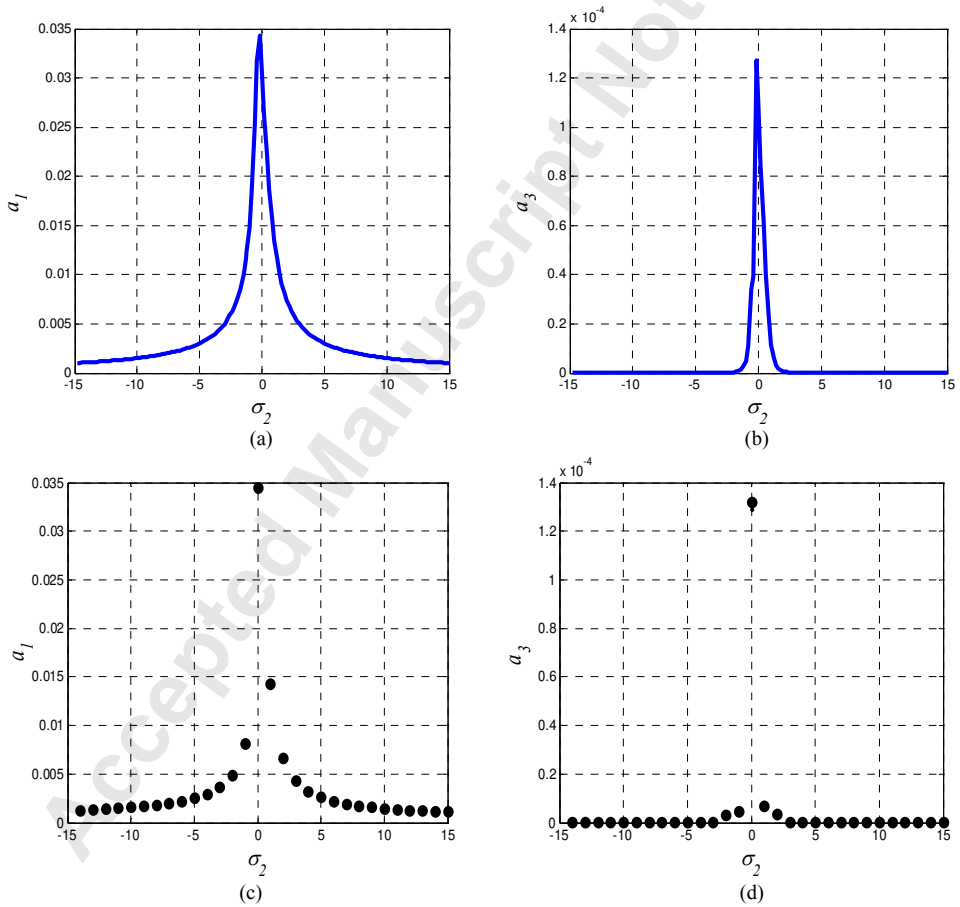

Fig. 3: Variation of the amplitudes a_1 and a_3 with the detuning parameter σ_2 for b_0=3.44μm, V_{DC}=10 *Volt*, V_{AC}=5 *Volt*, ξ=0.01, and σ_1=0: (a) and (b) using the perturbation method, and (c) and (b) using the long-time integration.

Next, we generate the variation of the modal amplitudes curves while varying the detuning parameter σ_2 near the first mode at V_{DC}=10 *Volt*. Note that at this specific DC load, the ratio between ω_1 and ω_3 is still around to 3. Figures 3a and 3b shows the variation of both first and third modes amplitude with the detuning parameter, using the method of multiple scales, for an AC load of 5 *Volt*. One can see clearly that the considered modes are behaving both linearly with an amplitude dominance of the first mode. Figures 3c and 3d compare the obtained frequency-response curves using the perturbation technique to those using a direct numerical integration of the ROM differential equations assuming four mode shapes. We notice excellent agreement between both approaches for the cases of Figs. 3a and 3c for the first mode amplitudes and Figs. 3b and 3d for the third mode amplitudes.

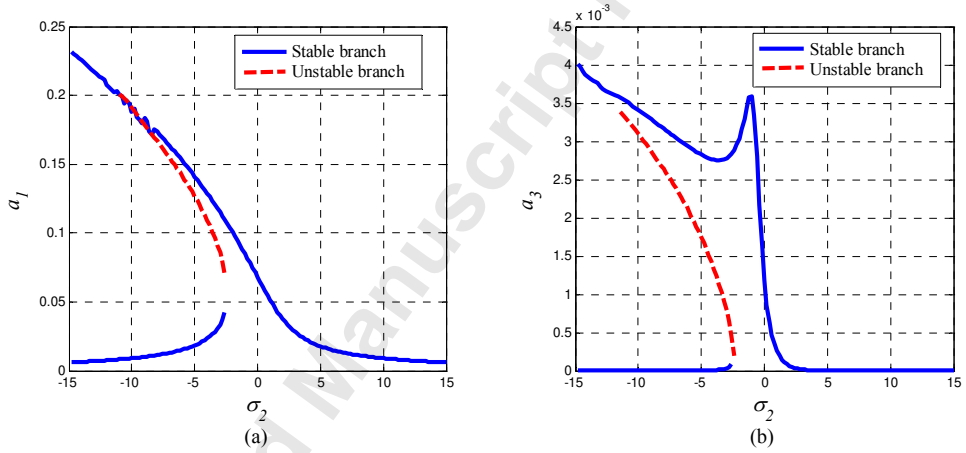

Fig. 4: Variation of the amplitudes a_1 and a_3 with the detuning parameter σ_2 for b_0=3.44μm, V_{DC}=10 *Volt*, V_{AC}=30 *Volt*, ξ=0.01, and σ_1=0.

Increasing further the AC load to 30 *Volt*, the dominant mode (first mode), Fig. 4a, starts to behave nonlinearly and is affected by the behavior of the other mode (the third mode), Fig. 4b, which has now a linear and a nonlinear part in its frequency response curve. The nonlinear part is created due to the nonlinear interaction between the modes, even though it turns out to be

weak due to the dominance in the amplitude of the first mode, as depicted in Fig. 3. This is an indication of internal resonance activation in the third mode.

ii) One-to-one internal resonance

Now, we focus on the one-to-one internal resonance case between the first symmetric and the second antisymmetric mode of the arch, which may occur when b_0= 6.32 μm, Fig. 2. We can see from Table 3 that the interaction coefficients (R_3 and R_8) are nonzero for this particular case, offering the possibility to have nonlinear interaction between the considered modes.

Table 3: The interaction coefficients S_{ij} and R_i for the case of one-to-one internal resonance between the m^{th} and n^{th} modes.

m	n	b_0	S_{mm}	S_{nn}	S_{mn}	S_{nm}	R_3	R_8
1	2	6.32	-1.32×10^4	-1.25×10^4	-2.57×10^4	-2.57×10^4	-1.32×10^4	-1.25×10^4

Next, we show the variation of the modal amplitudes curves while varying the detuning parameter σ_2 near the first mode at V_{DC}=5 *Volt*. Note here that we used an antisymmetric distribution of the electric load (half electrode configuration) since the considered modes are of antisymmetric type. We did this by multiplying the forcing term by *u(x-0.5)* where *u* is the unit-step function. Figure 5 shows the results for an AC load of 30 *Volt* and 0.01 damping ratio. Looking carefully at the perturbation method results, Figures 5a and 5b, we cannot recognize any possibility of internal resonance being activated since the considered modes are behaving both linearly with a dominance of the first mode amplitude. In the same figure, we compare the obtained frequency-response curves using the perturbation technique to those using a direct numerical time integration of the ROM differential equations assuming four mode shapes. We notice excellent agreement between both approaches for the cases of Figs. 5a and 5c for the first mode amplitudes and Figs. 5b and 5d for the second mode amplitudes.

Next, decreasing further the damping ratio to 0.001, we see that both modes start to interact nonlinearly, Fig. 6. Each curve has now linear and nonlinear part. Again, this is due to

the existence of multiple solutions, which leads to several jumps phenomena that could occur here for both modes while interacting. As σ_2 is swept gradually from negative values, the amplitude of the first mode starts to increase. As σ_2 approached zero, we have a linear increase for both modes, indicating resonance for both of them with slight amplitude dominance for the first mode. When σ_2 reaches values between 0.3 and 0.5, we see a drop for both amplitudes but with dominance of the second mode. Finally, as σ_2 passes 0.5, we see a nonlinear part being created for both resonances, which is due to the nonlinearity of the system indicating a possible activation of the one-to-one internal resonance.

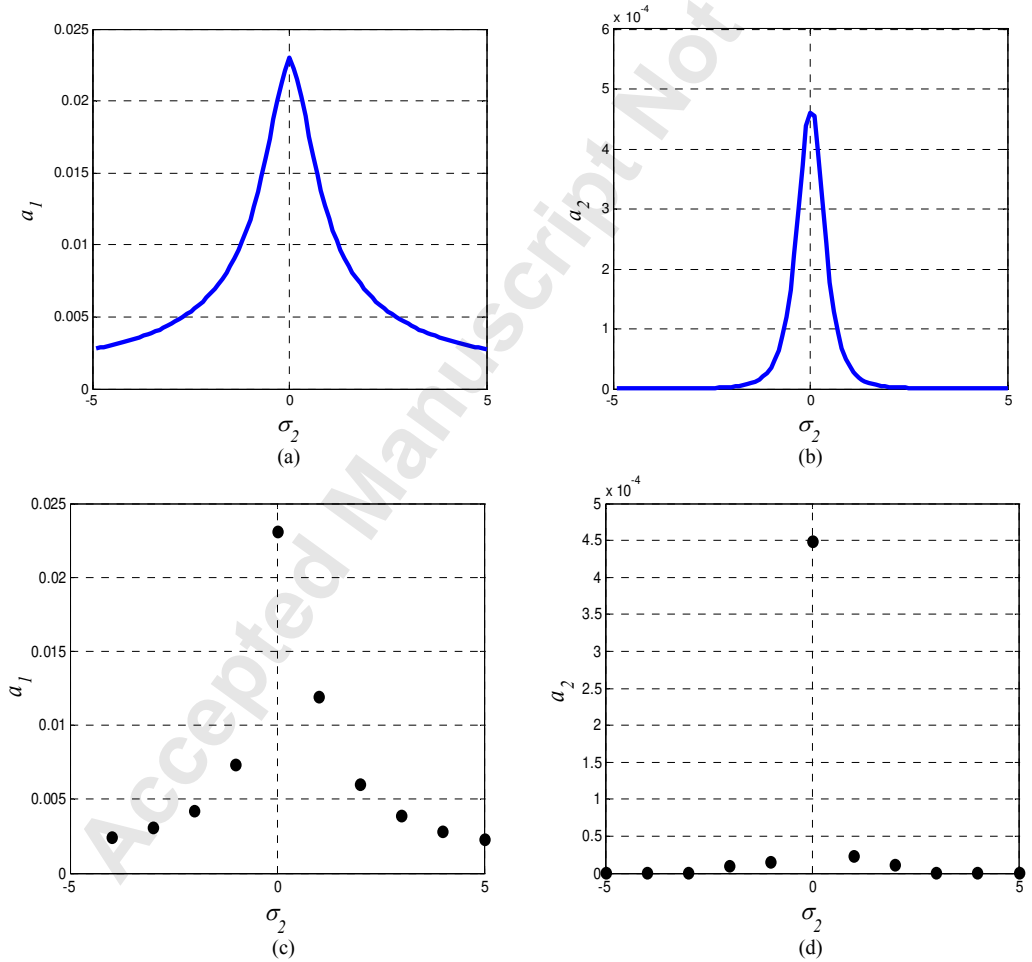

Fig. 5: Variation of the amplitudes a_1 and a_2 with the detuning parameter σ_2 for b_0=6.32 μm, V_{DC}=5 *Volt*, V_{AC}=30 *Volt*, ξ =0.01, and σ_1 =0: (a) and (b) using the perturbation method, and (c) and (d) using the long-time integration.

Journal of Computational and Nonlinear Dynamics. Received November 08, 2016;
Accepted manuscript posted May 24, 2017. doi:10.1115/1.4036815

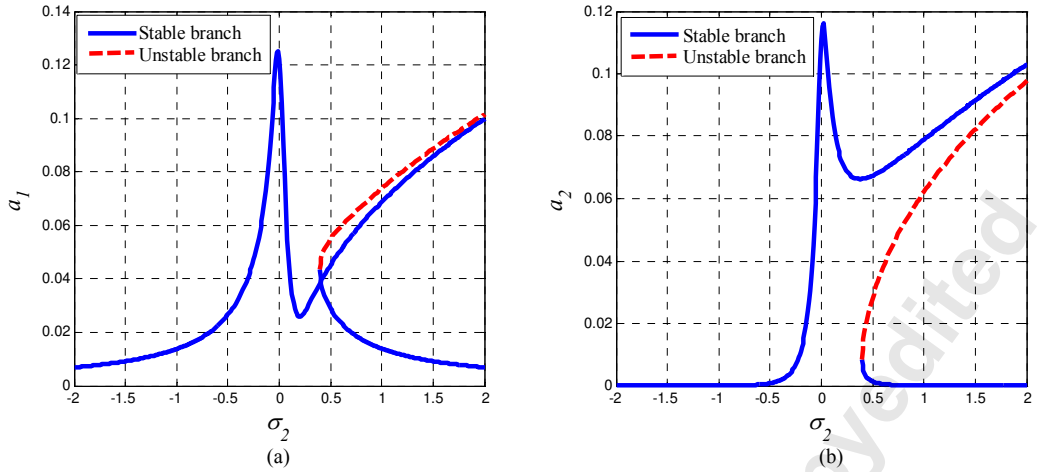

Fig. 6: Variation of the amplitudes a_1 and a_2 with the detuning parameter σ_2 for b_0=6.32 μm, V_{DC}=5 *Volt*, V_{AC}=30 *Volt*, ξ=0.001, and σ_1=0.

5. Conclusions

The possible activation of three-to-one and one-to-one internal resonances arising from the nonlinear modal interaction of arch shaped MEMS actuator was studied. The perturbation-technique of the method of multiple scales was employed to derive the nonlinear relation between the amplitude and exciting frequency and extract the complex dynamic behavior of the system. It was demonstrated that the energy can be interestingly exchanged between the successive modes of the structure for some values of initial rise. The theoretical methodology presented here can be potentially useful for a wide variety of applications employing internal resonances.

Appendix A

In this Appendix, we provide details on the applications of the method of multiple scales of the equations of motion, Eqs. (5) and (6) using the direct attack approach [47]. To this end, we define the following variables for the time scale (T_i) and its derivative:

$$T_0 = t, \quad D_0 = \frac{\partial}{\partial T_0}, \quad T_1 = \varepsilon\, t, \quad D_1 = \frac{\partial}{\partial T_1}, \quad T_2 = \varepsilon^2 t, \quad D_2 = \frac{\partial}{\partial T_2}, \tag{A1}$$

Next, we scale the damping coefficient *c* and the forcing amplitude V_{AC} so that the nonlinearity balances their effects in the modulation equations [47], hence

$$c = \varepsilon^2 c, \qquad V_{\mathrm{AC}} = \varepsilon^3 V_{\mathrm{AC}}, \tag{A2}$$

where ε is a bookkeeping parameter. We seek a solution in the following form

$$\begin{aligned} w(x,t,\varepsilon) &= w_s(x) + u(x,t) \\ &= w_s(x) + \varepsilon u_1(x,T_0,T_2) + \varepsilon^2 u_2(x,T_0,T_2) + \varepsilon^3 u_3(x,T_0,T_2) + \ldots, \end{aligned} \tag{A3}$$

where w_s is the static component of the arch deflection and *u* is its dynamic component.

For simplicity, we define

$$\Gamma\left(p(x), g(x)\right) = \int_0^1 \left[\, p'(x)\, g'(x)\right] dx, \tag{A4}$$

Substituting Eqs. (A1)-(A5) into Eqs. (5)-(6) and equating like powers of ε, we obtain:

- **Order ε^0: (the static equation)**

$$\begin{aligned} w_s^{iv} &= \alpha_1 \left[w_s'' + w_0''\right]\left[\Gamma(w_s, w_s) + 2\Gamma(w_s, w_0)\right] - \frac{\alpha_2 V_{DC}^2}{\left(1 + w_0 + w_s\right)^2}, \\ w_s(0) &= w_s(1) = 0, \qquad w_s'(0) = w_s'(1) = 0, \end{aligned} \tag{A5}$$

- **Order ε^1:**

$$\mathcal{L}(u_1)=0, \tag{A6}$$

where:

$$\mathcal{L}(u_1)=D_0^2u_1+u_1^{iv}-\alpha_1\left[\Gamma(w_s,w_s)+2\Gamma(w_s,w_0)\right]u_1''-2\alpha_1\left[w_s''+w_0''\right]\left[\Gamma(w_s,u_1)+\Gamma(w_0,u_1)\right]+ \\ -\frac{2\alpha_2V_{\mathrm{DC}}^2}{(1+w_0+w_s)^3}u_1,$$

- **Order ε^2:**

$$\mathcal{L}(u_2)=\alpha_1\Gamma(u_1,u_1)\left(w_s''+w_0''\right)+2\alpha_1\left[\Gamma(w_0,u_1)+\Gamma(w_s,u_1)\right]u_1''-\frac{3\alpha_2V_{\mathrm{DC}}^2}{(1+w_0+w_s)^4}u_1^2, \tag{A7}$$

- **Order ε^3:**

$$\begin{aligned}\mathcal{L}(u_3)=&\,2\alpha_1\Gamma(u_1,u_2)\left(w_s''+w_0''\right)+2\alpha_1\left[\Gamma(w_s,u_1)+\Gamma(w_0,u_1)\right]u_2'' \\ &+2\alpha_1\left[\Gamma(w_s,u_2)+\Gamma(w_0,u_2)\right]u_1''+\alpha_1\Gamma(u_1,u_1)u_1''-2D_0D_2u_1-cD_0u_1 \\ &-\frac{2\alpha_2V_{\mathrm{DC}}V_{\mathrm{AC}}\cos(\Omega t)}{(1+w_0+w_s)^2}-\frac{6\alpha_2V_{\mathrm{DC}}^2}{(1+w_0+w_s)^4}u_1u_2+\frac{4\alpha_2V_{\mathrm{DC}}^2}{(1+w_0+w_s)^5}u_1^3,\end{aligned} \tag{A8}$$

Because we suspect the activation of internal resonances for the investigated MEMS arch, we seek a second order uniform expansion for the solution of Eq. (A6) in the following form:

$$u_1(x,T_0,T_2)=A_n(T_2)e^{i\omega_nT_0}\phi_n(x)+A_m(T_2)e^{i\omega_mT_0}\phi_m(x)+cc, \tag{A9}$$

where $A_n(T_2)$ and $A_m(T_2)$ are complex-valued functions, ω_n, ω_m and $\phi_n(x)$, $\phi_m(x)$ are the natural frequencies and corresponding eigenfunctions respectively, and where the subscripts *m* and *n* indicate the modes involved in the internal resonance. "*cc*" in Eq. (A9) stands for the complex conjugates terms. Substituting Eq. (A9) into Eq. (A7), we obtain

$$\begin{aligned}\mathcal{L}(u_2) = {} & A_n^2 e^{2i\omega_n T_0} h_{1n}(x) + A_m^2 e^{2i\omega_m T_0} h_{1m}(x) + A_n \overline{A}_n h_{1n}(x) + A_m \overline{A}_m h_{1m}(x) \\ & + \left(A_n A_m e^{i(\omega_n+\omega_m)T_0} + A_n \overline{A}_m e^{i(\omega_n-\omega_m)T_0} \right) H_{nm}(x) + cc,\end{aligned} \tag{A10}$$

where

$$h_{1i}(x) = -\frac{3\alpha_2 V_{DC}^2}{(1+w_0+w_s)^4}\phi_i^2 + 2\alpha_1\left(\Gamma(w_s,\phi_i)+\Gamma(w_0,\phi_i)\right)\phi_i'' + \alpha_1\Gamma(\phi_i,\phi_i)\left(w_s'' + w_0''\right), \tag{A11}$$

$$\begin{aligned}H_{ij}(x) = {} & -\frac{6\alpha_2 V_{DC}^2}{(1+w_0+w_s)^4}\phi_i\phi_j + 2\alpha_1\left(\Gamma(w_s,\phi_i)+\Gamma(w_0,\phi_i)\right)\phi_j'' \\ & + 2\alpha_1\left(\Gamma(w_s,\phi_j)+\Gamma(w_0,\phi_j)\right)\phi_i'' + 2\alpha_1\Gamma(\phi_i,\phi_j)\left(w_s'' + w_0''\right),\end{aligned} \tag{A12}$$

A particular solution of Eq. (A10) can be basically expressed as:

$$\begin{aligned}u_2(x,T_0,T_2) = {} & \psi_{1n}(x) A_n^2(T_2) e^{2i\omega_n T_0} + \psi_{1m}(x) A_m^2(T_2) e^{2i\omega_m T_0} \\ & + \psi_3(x) A_n(T_2) A_m(T_2) e^{i(\omega_n+\omega_m)T_0} + \psi_4(x) A_n(T_2)\overline{A}_m(T_2) e^{i(\omega_n-\omega_m)T_0} \\ & + \psi_{2n}(x) A_n(T_2)\overline{A}_n(T_2) + \psi_{2m}(x) A_m(T_2)\overline{A}_m(T_2) + cc,\end{aligned} \tag{A13}$$

where

$$H\left(\psi_{1i}(x), 2\omega_i\right) = h_{1i}(x), \tag{A14}$$

$$H\left(\psi_{2i}(x), 0\right) = h_{1i}(x), \tag{A15}$$

$$H\left(\psi_3(x), \omega_n+\omega_m\right) = H_{nm}(x), \tag{A16}$$

$$H\left(\psi_4(x), \omega_n-\omega_m\right) = H_{nm}(x), \tag{A17}$$

and where the operator H is defined by the following equation:

$$\begin{aligned}H(f,\omega) = {} & f^{iv} - \omega^2 f - 2\alpha_1\left(w_0'' + w_s''\right)\left[\Gamma(f,w_0)+\Gamma(f,w_s)\right] \\ & -\alpha_1\left[\Gamma(w_s,w_s)+2\Gamma(w_0,w_s)\right]f'' - \frac{2\alpha_2 V_{DC}^2}{(1+w_0+w_s)^3} f,\end{aligned} \tag{A18}$$

Next we obtain the perturbation solutions for two different cases of internal resonances: three-too-one and one-to-one cases.

i) Three-to-one internal resonance case ($\omega_n \approx 3\omega_m$)

Substituting Eqs. (A9) and (A13) into Eq. (A8) and considering the case where $\omega_n \approx 3\omega_m$ and $\Omega \approx \omega_n$ or ω_m, we obtain

$$\begin{aligned}\mathcal{L}(u_3) = &\left[-i\omega_n\left(2A_n' + \hat{c}A_n\right)\phi_n(x) + \chi_{1n}(x)A_n^2\overline{A}_n + \chi_{nm}(x)A_nA_m\overline{A}_m\right]e^{i\omega_nT_0}\\ &+\left[-i\omega_m\left(2A_m' + \hat{c}A_m\right)\phi_m(x) + \chi_{1m}(x)A_m^2\overline{A}_m + \chi_{mn}(x)A_mA_n\overline{A}_n\right]e^{i\omega_mT_0}\\ &+\chi_5(x)A_m^3e^{3i\omega_mT_0} + \chi_6(x)A_n\overline{A}_m^2e^{i(\omega_n-2\omega_m)T_0} + \overline{F}(x)e^{i\Omega T_0} + cc + NST,\end{aligned} \tag{A19}$$

where "NST" refers for non-secular terms, and where the forcing term $\overline{F}$ is defined by

$$\overline{F}(x) = -\frac{2\alpha_2V_{\mathrm{DC}}V_{\mathrm{AC}}}{\left(1+w_0+w_s\right)^2}, \tag{A20}$$

and where:

$$\begin{aligned}\chi_{1i}(x) = &\alpha_1\phi_i''\left[3\Gamma(\phi_i,\phi_i) + 2\Gamma(w_s,\psi_{1i}) + 2\Gamma(w_0,\psi_{1i}) + 4\Gamma(w_s,\psi_{2i}) + 4\Gamma(w_0,\psi_{2i})\right] +\\ &+\alpha_1\left[w_s'' + w_0''\right]\left[2\Gamma(\phi_i,\psi_{1i}) + 4\Gamma(\phi_i,\psi_{2i})\right] +\\ &+2\alpha_1\left[\psi_{1i}'' + 2\psi_{2i}''\right]\left[\Gamma(\phi_i,w_s) + \Gamma(\phi_i,w_0)\right] +\\ &+\frac{12\alpha_2V_{\mathrm{DC}}^2}{\left(1+w_0+w_s\right)^5}\phi_i^3 - \frac{6\alpha_2V_{\mathrm{DC}}^2}{\left(1+w_0+w_s\right)^4}\phi_i\psi_{1i} - \frac{12\alpha_2V_{\mathrm{DC}}^2}{\left(1+w_0+w_s\right)^4}\phi_i\psi_{2i},\end{aligned} \tag{A21}$$

$$\begin{aligned}\chi_{ij}(x) = &\alpha_1\phi_j''\left[4\Gamma(\phi_i,\phi_j) + 2\Gamma(w_0,\psi_3) + 2\Gamma(w_s,\psi_3) + 2\Gamma(w_0,\psi_4) + 2\Gamma(w_s,\psi_4)\right]\\ &\alpha_1\phi_i''\left[2\Gamma(\phi_j,\phi_j) + 4\Gamma(w_0,\psi_{2j}) + 4\Gamma(w_s,\psi_{2j})\right]\\ &+\alpha_1\left[w_s'' + w_0''\right]\left[2\Gamma(\phi_j,\psi_3) + 2\Gamma(\phi_j,\psi_4) + 4\Gamma(\phi_i,\psi_{2j})\right]\\ &+2\alpha_1\left[\psi_3'' + \psi_4''\right]\left[\Gamma(\phi_j,w_s) + \Gamma(\phi_j,w_0)\right]\\ &+4\alpha_1\psi_{2j}''\left[\Gamma(\phi_i,w_s) + \Gamma(\phi_i,w_0)\right]\\ &+\frac{24\alpha_2V_{\mathrm{DC}}^2}{\left(1+w_0+w_s\right)^5}\phi_i\phi_j^2 - \frac{6\alpha_2V_{\mathrm{DC}}^2}{\left(1+w_0+w_s\right)^4}\left(\psi_3\phi_j + \psi_4\phi_j + 2\psi_{2j}\phi_i\right),\end{aligned} \tag{A22}$$

$$\begin{aligned}\chi_5(x) = &\alpha_1\phi_m''\left[\Gamma(\phi_m,\phi_m) + 2\Gamma(w_0,\psi_{1m}) + 2\Gamma(w_s,\psi_{1m})\right] + 2\alpha_1\left[w_s'' + w_0''\right]\Gamma(\phi_m,\psi_{1m})\\ &+2\alpha_1\psi_{1m}''\left[\Gamma(\phi_m,w_0) + \Gamma(\phi_m,w_s)\right] + \frac{4\alpha_2V_{\mathrm{DC}}^2}{\left(1+w_0+w_s\right)^5}\phi_m^3 - \frac{6\alpha_2V_{\mathrm{DC}}^2}{\left(1+w_0+w_s\right)^4}\phi_m\psi_{1m},\end{aligned} \tag{A23}$$

$$\begin{aligned}\chi_6(x) &= \alpha_1\phi_m''\left[2\Gamma(\phi_n,\phi_m)+2\Gamma(w_0,\psi_4)+2\Gamma(w_s,\psi_4)\right]\\ &+\alpha_1\phi_n''\left[\Gamma(\phi_m,\phi_m)+2\Gamma(w_0,\psi_{1m})+2\Gamma(w_s,\psi_{1m})\right]\\ &+\alpha_1\left[w_s''+w_0''\right]\left[2\Gamma(\phi_n,\psi_{1m})+2\Gamma(\phi_m,\psi_4)\right]+\alpha_1\psi_4''\left[2\Gamma(\phi_m,w_0)+2\Gamma(\phi_m,w_s)\right]\\ &+\alpha_1\psi_{1m}''\left[2\Gamma(\phi_n,w_0)+2\Gamma(\phi_n,w_s)\right]\\ &+\frac{12\alpha_2V_{\mathrm{DC}}^2}{(1+w_0+w_s)^5}\phi_n\phi_m^2-\frac{6\alpha_2V_{\mathrm{DC}}^2}{(1+w_0+w_s)^4}\phi_m\psi_4-\frac{6\alpha_2V_{\mathrm{DC}}^2}{(1+w_0+w_s)^4}\phi_n\psi_{1m},\end{aligned} \tag{A24}$$

Next, to describe the nearness of ω_n to $3\omega_m$ and Ω to either ω_m, we introduce the following detuning parameters σ_1 and σ_2 defined by

$$\omega_n = 3\omega_m + \varepsilon^2\sigma_1, \text{ and } \Omega = \omega_m + \varepsilon^2\sigma_2, \tag{A25}$$

Because the homogeneous problem governing u_3, Eq. (A19), has a nontrivial solution, the corresponding nonhomogeneous problem has a solution only if the right-hand side of Eq. (A19) is orthogonal to every solution of the adjoint homogeneous problem governing u_3. Since this problem is self-adjoint, the adjoints are given by $\phi_j(x)e^{\pm i\omega_j T_0}$. Requiring that the right-hand side of Eq. (A19) be orthogonal to $\phi_n(x)e^{-i\omega_n T_0}$ and $\phi_m(x)e^{-i\omega_m T_0}$ and using Eq. (A25), we obtain the following solvability conditions for the case of three-to-one internal resonance

$$i\omega_n\left(2A_n'+\hat{c}A_n\right) = S_{nn}A_n^2\overline{A}_n + S_{nm}A_nA_m\overline{A}_m + \Lambda_nA_m^3e^{-i\sigma_1T_2} + f_n\delta_{in}e^{i\sigma_2T_2}, \tag{A26}$$

$$i\omega_m\left(2A_m'+\hat{c}A_m\right) = S_{mm}A_m^2\overline{A}_m + S_{mn}A_mA_n\overline{A}_n + \Lambda_mA_n\overline{A}_m^2e^{i\sigma_1T_2} + f_m\delta_{im}e^{i\sigma_2T_2}, \tag{A27}$$

where :

$$f_k = \int_0^1 \overline{F}(x)\phi_k(x)dx, \tag{A28}$$

$$S_{kk} = \int_0^1 \chi_{1k}(x)\phi_k(x)dx, \tag{A29}$$

$$S_{jk}=\int_0^1 \chi_{jk}\left(x\right)\phi_j\left(x\right)dx,\ \ j\neq k, \tag{A30}$$

$$\Lambda_n=\int_0^1 \chi_5\left(x\right)\phi_n\left(x\right)dx,\ \ \Lambda_m=\int_0^1 \chi_6\left(x\right)\phi_m\left(x\right)dx, \tag{A31}$$

Afterward, we express the A_i in the polar form $A_i=a_i e^{i\beta_i}/2$, where $a_i=a_i\left(T_2\right)$ and $\beta_i=\beta_i\left(T_2\right)$ are real-valued functions, representing, respectively, the amplitude and phase of the response of each A_i. Substituting for the expression of A_i into Eqs. (A26) and (A27) and letting $\gamma_1=\sigma_1 T_2-3\beta_m+\beta_n$, and $\gamma_{2m}=\sigma_2 T_2-\beta_m$, where $a_i=a_i\left(T_2\right)$ and $\beta_i=\beta_i\left(T_2\right)$ are real-valued functions, representing, respectively, the amplitude and phase of the response of the i^{th} mode, we obtain the following modulation equations governing the modal amplitudes and phases respectively:

$$a_n'=-\hat{c}\frac{1}{2}a_n-\frac{\Lambda_n}{8\omega_n}a_m^3\sin\left(\gamma_1\right), \tag{A32}$$

$$a_n\left(\gamma_1'-3\gamma_{2m}'\right)=a_n\left(\sigma_1-3\sigma_2\right)-\frac{S_{nn}}{8\omega_n}a_n^3-\frac{S_{nm}}{8\omega_n}a_n a_m^2-\frac{\Lambda_n}{8\omega_n}a_m^3\cos\left(\gamma_1\right), \tag{A33}$$

$$a_m'=-\hat{c}\frac{1}{2}a_m+\frac{\Lambda_m}{8\omega_m}a_n a_m^2\sin\left(\gamma_1\right)+\frac{f_m}{\omega_m}\sin\left(\gamma_{2m}\right), \tag{A34}$$

$$a_m\gamma_{2m}'=-a_m\sigma_2+\frac{S_{mm}}{8\omega_m}a_m^3+\frac{S_{mn}}{8\omega_m}a_m a_n^2+\frac{\Lambda_m}{8\omega_m}a_n a_m^2\cos\left(\gamma_1\right)+\frac{f_m}{\omega_m}\cos\left(\gamma_{2m}\right), \tag{A35}$$

ii) One-to-one internal resonance case ($\omega_n\approx\omega_m$)

Note here that the above analysis of the three-to-one internal resonance up to Eq. (A18) holds for the present case. However, instead of Eq. (A19), we have the following solution for the

cases of one-to-one internal resonance, assuming considering the case where $\omega_n \approx \omega_m$ and $\Omega \approx \omega_n$ or ω_m:

$$\begin{aligned}\mathcal{L}(u_3) = &\left[-i\omega_n\left(2A_n' + \hat{c}A_n\right)\phi_n(x) + \chi_{1n}(x)A_n^2\overline{A}_n + \chi_{nm}(x)A_nA_m\overline{A}_m\right]e^{i\omega_nT_0}\\ &+\left[-i\omega_m\left(2A_m' + \hat{c}A_m\right)\phi_m(x) + \chi_{1m}(x)A_m^2\overline{A}_m + \chi_{mn}(x)A_mA_n\overline{A}_n\right]e^{i\omega_mT_0}\\ &+\chi_6(x)A_m^2\overline{A}_ne^{i(2\omega_m-\omega_n)T_0} + \chi_7(x)A_n^2\overline{A}_me^{i(2\omega_n-\omega_m)T_0} + \overline{F}(x)e^{i\Omega T_0} + cc + NST,\end{aligned} \tag{A36}$$

where the functions $\chi_{1i}(x)$, $\chi_{ij}(x)$, and $\chi_6(x)$ are defined in Eqs. (A21), (A22), and (A24) respectively, and where

$$\begin{aligned}\chi_7(x) = &\alpha_1\phi_n''\left[2\Gamma(\phi_n,\phi_m) + 2\Gamma(w_0,\psi_4) + 2\Gamma(w_s,\psi_4)\right]\\ &+\alpha_1\phi_m''\left[\Gamma(\phi_n,\phi_n) + 2\Gamma(w_0,\psi_{1n}) + 2\Gamma(w_s,\psi_{1n})\right]\\ &+\alpha_1\left[w_s'' + w_0''\right]\left[2\Gamma(\phi_m,\psi_{1n}) + 2\Gamma(\phi_n,\psi_4)\right] + \alpha_1\psi_4''\left[2\Gamma(\phi_n,w_0) + 2\Gamma(\phi_n,w_s)\right]\\ &+\alpha_1\psi_{1n}''\left[2\Gamma(\phi_m,w_0) + 2\Gamma(\phi_m,w_s)\right]\\ &+\frac{12\alpha_2V_{\mathrm{DC}}^2}{(1+w_0+w_s)^5}\phi_m\phi_n^2 - \frac{6\alpha_2V_{\mathrm{DC}}^2}{(1+w_0+w_s)^4}\phi_n\psi_4 - \frac{6\alpha_2V_{\mathrm{DC}}^2}{(1+w_0+w_s)^4}\phi_m\psi_{1n},\end{aligned} \tag{A37}$$

Now, to describe the nearness of ω_n to ω_m and Ω to ω_m, we introduce the detuning parameters σ_1 and σ_2 defined by

$$\omega_n = \omega_m + \varepsilon^2\sigma_1, \text{ and } \Omega = \omega_m + \varepsilon^2\sigma_2, \tag{A38}$$

Similar to the three-to-one internal resonance case, we demand that the right-hand side of Eq. (A36) be orthogonal to $\phi_n(x)e^{-i\omega_nT_0}$ and $\phi_m(x)e^{-i\omega_mT_0}$ and then using Eq. (A38) along with the polar form of each A_i, we obtain the following modulations equations

$$\begin{aligned}a_n' = &-\frac{\hat{c}}{2}a_n - \frac{R_1}{8\omega_n}a_m^3\sin(\gamma_1) - \frac{R_2}{8\omega_n}a_n^2a_m\sin(\gamma_1) +\\ &-\frac{R_3}{8\omega_n}a_m^2a_n\sin(2\gamma_1) + \frac{R_4}{8\omega_n}a_n^3\sin(\gamma_1);\end{aligned} \tag{A39}$$

$$a_n\left(\gamma_1'-\gamma_{2m}'\right)=a_n\left(\sigma_1-\sigma_2\right)-\frac{S_{nn}}{8\omega_n}a_n^3-\frac{S_{nm}}{8\omega_n}a_n a_m^2-\frac{R_1}{8\omega_n}a_m^3\cos\left(\gamma_1\right)+$$
$$-\frac{R_2}{8\omega_n}a_n^2a_m\cos\left(\gamma_1\right)-\frac{R_3}{8\omega_n}a_m^2a_n\cos\left(2\gamma_1\right)-\frac{R_4}{8\omega_n}a_n^3\cos\left(\gamma_1\right); \tag{A40}$$

$$a_m'=-\frac{\hat{c}}{2}a_m+\frac{R_5}{8\omega_m}a_n^3\sin\left(\gamma_1\right)+\frac{R_6}{8\omega_m}a_m^2a_n\sin\left(\gamma_1\right)+$$
$$-\frac{R_7}{8\omega_m}a_n^2a_m\sin\left(2\gamma_1\right)+\frac{R_8}{8\omega_m}a_m^3\sin\left(\gamma_1\right)+\frac{f_m\delta_{im}}{\omega_m}\sin\left(\gamma_{2m}\right); \tag{A41}$$

$$a_m\gamma_{2m}'=-a_m\sigma_2-\frac{S_{mm}}{8\omega_m}a_m^3-\frac{S_{mn}}{8\omega_m}a_m a_n^2-\frac{R_5}{8\omega_m}a_n^3\cos\left(\gamma_1\right)-\frac{R_6}{8\omega_m}a_m^2a_n\cos\left(\gamma_1\right)+$$
$$-\frac{R_7}{8\omega_m}a_m^2a_n\cos\left(2\gamma_1\right)-\frac{R_8}{8\omega_m}a_n^2a_m\cos\left(\gamma_1\right)-\frac{f_m\delta_{im}}{\omega_m}\cos\left(\gamma_{2m}\right); \tag{A42}$$

where:

$$\gamma_1=\sigma_1T_2-\beta_m+\beta_n,\qquad \gamma_{2m}=\sigma_2T_2-\beta_m, \tag{A43}$$

and:

$$R_1=\int_0^1\chi_{1m}\left(x\right)\phi_n\left(x\right)dx,\ \ R_2=\int_0^1\chi_{mn}\left(x\right)\phi_n\left(x\right)dx,\ R_3=\int_0^1\chi_6\left(x\right)\phi_n\left(x\right)dx,$$
$$R_4=\int_0^1\chi_7\left(x\right)\phi_n\left(x\right)dx,\ \ R_5=\int_0^1\chi_{1n}\left(x\right)\phi_m\left(x\right)dx,\ \ R_6=\int_0^1\chi_{nm}\left(x\right)\phi_m\left(x\right)dx, \tag{A44}$$
$$R_7=\int_0^1\chi_6\left(x\right)\phi_m\left(x\right)dx,\ R_8=\int_0^1\chi_7\left(x\right)\phi_m\left(x\right)dx,$$

Finally, and for both types of investigated internal resonances, substituting Eqs. (A9) and (A13) into Eq. (A3) and setting $\varepsilon=1$, we obtain, to the second-order approximation, the following response of the MEMS arch to the DC and AC harmonic excitation:

$$w(x,t) = w_s(x) + a_n \cos(\omega_n t + \beta_n)\phi_n(x) + a_m \cos(\omega_m t + \beta_m)\phi_m(x) +$$
$$+\frac{1}{2}a_n{}^2\left[\cos 2(\omega_n t + \beta_n)\psi_{in}(x) + \psi_{2n}(x)\right] + \frac{1}{2}a_m{}^2\left[\cos 2(\omega_m t + \beta_m)\psi_{im}(x) + \psi_{2m}(x)\right] + \quad \text{(A45)}$$
$$+\frac{1}{2}a_n a_m\left[\cos\left((\omega_n + \omega_m)t + \beta_n + \beta_m\right)\psi_3(x)\right] + \cos\left((\omega_n - \omega_m)t + \beta_n - \beta_m\right)\psi_4(x) + \ldots,$$

Acknowledgment

This research was supported by the National Science Foundation NSF CAREER grant # 0846775.

References:

[1] S. Malihi, Y.T. Beni, H. Golestanian, Dynamic pull-in stability of torsional nano/micromirrors with size-dependency, squeeze film damping and van der Waals effect, Optik - International Journal for Light and Electron Optics 128 (2017) 156-171.
[2] M. Shojaeian, Y.T. Beni, H. Ataei, Electromechanical buckling of functionally graded electrostatic nanobridges using strain gradient theory, Acta Astronautica 118 (2016) 62-71.
[3] F. Marotti de Sciarra, R. Barretta, A gradient model for Timoshenko nanobeams, Physica E: Low-dimensional Systems and Nanostructures 62 (2014) 1-9.
[4] M. Canadija, R. Barretta, F. Marotti de Sciarra, A gradient elasticity model of Bernoulli–Euler nanobeams in non-isothermal environments, European Journal of Mechanics - A/Solids 55 (2016) 243-255.
[5] R. Barretta, M. Čanadija, F. Marotti de Sciarra, A higher-order Eringen model for Bernoulli–Euler nanobeams. Archive of Applied Mechanics 86(3) (2016) 483-495.
[6] B. Akgöz, Ö. Civalek, Mechanical analysis of isolated microtubules based on a higher-order shear deformation beam theory, Composite Structures 118 (2014) 9-18.
[7] F. Ebrahimi, M.R. Barati, Size-dependent thermal stability analysis of graded piezomagnetic nanoplates on elastic medium subjected to various thermal environments, Applied Physics A 122(10) (2016) 910.
[8] M. Shaat, M. Akbarzadeh Khorshidi, A. Abdelkefi, M. Shariati, Modeling and Vibration Characteristics of Cracked Nano-Beams Made of Nanocrystalline Materials, International Journal of Mechanical Sciences 115–116 (2016) 574-585.
[9] H.M. Ouakad, M.I. Younis. (2010). Nonlinear The dynamic behavior of MEMS arch resonators actuated electrically, International Journal of Non-Linear Mechanics 45(7) 704-713.
[10] N.-C. Tsai, C.-Y. Sue, C.-C. Lin, Design and dynamics of an innovative micro gyroscope against coupling effects, Microsystem Technologies 14(3) (2008) 295-306.
[11] R. Sanchez, P. Renard, Design of a micro-satellite for precise formation flying demonstration, Acta Astronautica 59(8–11) (2006) 862-872.
[12] C. Comi, A. Corigliano, A. Ghisi, S. Zerbini, A resonant micro accelerometer based on electrostatic stiffness variation, Meccanica 48(8) (2013) 1893-1900.
[13] S.K. Yoo, J.H. Lee, S.-S. Yun, M.B. Gu, J.H. Lee, Fabrication of a bio-MEMS based cell-chip for toxicity monitoring, Biosens Bioelectron 22(8) (2007) 1586-1592.
[14] N.-J. Choi, Y.-S. Lee, J.-H. Kwak, J.-S. Park, K.-B. Park, K.-S. Shin, H.-D. Park, J.-C. Kim, J.-S. Huh, D.-D. Lee, Chemical warfare agent sensor using MEMS structure and thick film fabrication method, Sensors and Actuators B: Chemical 108(1–2) (2005) 177-183.
[15] M. Hafiz, L. Kosuru, A. Ramini, K. Chappanda, M. Younis, In-Plane MEMS Shallow Arch Beam for Mechanical Memory, Micromachines 7(10) (2016) 191.
[16] M.A.A. Hafiz, L. Kosuru, M.I. Younis, Microelectromechanical reprogrammable logic device, Nature Communications 7 (2016) 11137.
[17] A. Y. T. Leung, T. C. Fung, Non-linear steady state vibration and dynamic snap through of shallow arch beams, Earthquake Engineering & Structural Dynamics 19 (1990) 409-430.
[18] L.-Q. Chen, W.-A. Jiang, Internal Resonance Energy Harvesting, Journal of Applied Mechanics 82 (2015) 031004.

[19] K. Das, R.C. Batra, Symmetry breaking, snap-through and pull-in instabilities under dynamic loading of microelectromechanical shallow arches, Smart Materials and Structures 18(11) (2009) 115008.
[20] H.M. Ouakad, An Electrostatically Actuated MEMS Arch Band-Pass Filter, Shock and Vibration 20(4) (2013).
[21] S.A. Alkharabsheh, M.I. Younis, Statics and Dynamics of MEMS Arches Under Axial Forces, Journal of Vibration and Acoustics 135(2) (2013) 021007-021007.
[22] A.H. Nayfeh, S.A. Emam, Exact solution and stability of postbuckling configurations of beams, Nonlinear Dyn. 54 (2008) 395–408.
[23] A. H. Nayfeh, and B. Balachandran. "Modal interactions in dynamical and structural systems." Appl. Mech. Rev 42, no. 11 (1989): 175-201.
[24] B. Balachandran, and A. H. Nayfeh. "Nonlinear oscillations of a harmonically excited composite structure." Composite Structures 16, no. 4 (1990): 323-339.
[25] S.A. Alkharabsheh, M.I. Younis, Dynamics of MEMS Arches of Flexible Supports, Journal of Microelectromechanical Systems 22(1) (2013) 216-224.
[26] H.M. Ouakad, M.I. Younis, On using the dynamic snap-through motion of MEMS initially curved microbeams for filtering applications, Journal of Sound and Vibration 333(2) (2014) 555-568.
[27] M.H. Ghayesh, H. Farokhi, G. Alici, Internal Energy Transfer in Dynamical Behavior of Slightly Curved Shear Deformable Microplates, Journal of Computational and Nonlinear Dynamics 11(4) (2015) 041002-041002.
[28] L. Medina, R. Gilat, S. Krylov, Latching in bistable electrostatically actuated curved micro beams, International Journal of Engineering Science 110 (2017) 15-34.
[29] Antonio, D. et. al. Frequency stabilization in nonlinear micromechanical oscillators. Nature Communications 3, 806, doi:10.1038/ncomms1813 (2012)
[30] Srinil, N. & Rega, G. Two-to-one resonant multi-modal dynamics of horizontal/inclined cables. Part II: Internal resonance activation, reducedorder models and nonlinear normal modes. Nonlinear Dyn. 48(3), 253–274, doi: 10.1007/s11071-006-9087-z (2007).
[31] Chen, L. Q. et. al., Internal resonance in forced vibration of coupled cantilevers subjected to magnetic interaction. J. of Sound and vibration.354,196–218 (2015).
[32] Westra, H.J.R. et. al., Modal interactions of flexural and torsional vibrations in a microcantilever. Ultramicroscopy. 120, 41–47 (2012).
[33] Chin, C. & Nayfeh, A., Three-to-one internal resonances in parametrically excited hinged-clamped beams. Nonlinear Dyn. 20, 131–158 (1999).
[34] Nayfeh, A. H. et. al. On nonlinear normal modes of systems with internal resonance. J. of Vibration and Acoustics. 118, 340-345 (1996).
[35] Malhotral, N. & Namachchivaya, N., Chaotic motion of shallow arch structures under 1:1 internal resonance. J. Eng. Mech. 123(6) 620-627 (1997).
[36] Tien, W. et. al. Non-linear dynamics of a shallow arch under periodic excitation-II. 1: 1 internal resonance. Int. J. Non-linear Mech. 29(3) 367-386 (1994).
[37] Nayfeh, A. et. al. Nonlinear normal modes of buckled beams: three-to-one and one-to-one internal resonances. Nonlinear dyn. 18, 253–273 (1999).
[38] El-Bassiouny, A. F., Kamel, M. M., & Abdel-Khalik, A. (2003). Two-to-one internal resonances in nonlinear two degree of freedom system with parametric and external excitations. Mathematics and computers in simulation, 63(1), 45-56.
[39] El-Bassiouny, A. F. Three-to-one internal resonance in the nonlinear oscillation of shallow arch. Physica Scripta. 72, 439–450 (2005)
[40] Bi, Q. & Dai, H. Analysis of non-linear dynamics and bifurcations of a shallow arch subjected to periodic excitation with internal resonance. J. of Sound and Vibration 233(4) 557-571, doi:10.1006/jsvi.1999.2813 (2000).
[41] A. H. Nayfeh, P. F. Pai, Linear and Nonlinear Structural Mechanics, John Wiley & Sons, New York, 2004.
[42] RC. Batra, M. Porfiri, Spinello D. Capacitance estimate for electrostatically actuated narrow microbeams. Micro Nano Lett. 1(2) 2006 71–73.
[43] Batra RC, Porfiri M, Spinello D. Electromechanical model of electrically actuated narrow microbeams. J Microelectromechanical Syst. 15(5) 2006 1175–1189.
[44] A.H., Nayfeh, Nonlinear Interactions, New-York, Wiley Interscience, United-States, 2000.
[45] A. Tondl, T. Ruigrock, F. Verhulst, R. Nabergoj, Autoparametric Resonance in Mechanical Systems, Cambridge University Press, Cambridge, United Kingdom, 2000.
[46] A.H. Nayfeh, D.T. Mook, Nonlinear Oscillations, New-York, Wiley Interscience, United-States, 1995.

[47] M.I. Younis, A.H. Nayfeh, A study of the nonlinear response of a resonant microbeam to an electric actuation, Nonlinear Dyn. 31 (2003) 91-117.
[48] A. H. Nayfeh. and B. Balachandran. Applied Nonlinear Dynamics, Wiley, New York, 1995.